

# Light Chiral Dark Sector

Keisuke Harigaya<sup>1,2</sup> and Yasunori Nomura<sup>1,2</sup>

<sup>1</sup>*Department of Physics, University of California, Berkeley, California 94720, USA*

<sup>2</sup>*Theoretical Physics Group, Lawrence Berkeley National Laboratory, Berkeley, California 94720, USA*

An interesting possibility for dark matter is a scalar particle of mass of order  $10 \text{ MeV} - 1 \text{ GeV}$ , interacting with a  $U(1)$  gauge boson (dark photon) which mixes with the photon. We present a simple and natural model realizing this possibility. The dark matter arises as a composite pseudo Nambu-Goldstone boson (dark pion) in a non-Abelian gauge sector, which also gives a mass to the dark photon. For a fixed non-Abelian gauge group,  $SU(N)$ , and a  $U(1)$  charge of the constituent dark quarks, the model has only three free parameters: the dynamical scale of the non-Abelian gauge theory, the gauge coupling of the dark photon, and the mixing parameter between the dark and standard model photons. In particular, the gauge symmetry of the model does not allow any mass term for the dark quarks, and stability of the dark pion is understood as a result of an accidental global symmetry. The model has a significant parameter space in which thermal relic dark pions comprise all of the dark matter, consistently with all experimental and cosmological constraints. In a corner of the parameter space, the discrepancy of the muon  $g - 2$  between experiments and the standard model prediction can also be ameliorated due to a loop contribution of the dark photon. Smoking-gun signatures of the model include a monophoton signal from the  $e^+e^-$  collision into a photon and a “dark rho meson.” Observation of two processes in  $e^+e^-$  collision, the mode into the dark photon and that into the dark rho meson, would provide strong evidence for the model.

## I. INTRODUCTION

The identity of the dark matter of the universe is unknown. An interesting possibility is that it is a relatively light particle of mass of order  $10 \text{ MeV} - 1 \text{ GeV}$ , interacting with the standard model particles through a  $U(1)$  gauge boson (dark photon) that mixes with the photon [1–3]. This avoids stringent constraints from dark matter direct detection experiments [4, 5] while still allows for understanding the current dark matter abundance as the thermal relic from the early universe, if the mixing between the dark and standard model photons is adequately suppressed.

This potentially elegant scenario, however, suffers from the issue of naturalness. First of all, if the dark matter is a fermion, then the constraint on its late annihilations from observations of the cosmic microwave background excludes the scenario [6–8]. This (essentially) forces the dark matter to be a scalar, in which case the constraint is avoided because of the  $p$ -wave suppression of the annihilation cross section [9]. This, however, raises the question: why do we have such a light scalar? This is puzzling, especially given that a scalar mass is generally unstable under quantum corrections. A similar question can also be raised for the dark photon, whose mass must be in the same range as the scalar mass for phenomenological reasons.

In this paper, we present a simple model addressing this issue, in which the dark matter arises as a “dark pion” of new gauge interactions with the dynamical scale  $\Lambda \approx O(10 \text{ MeV} - 1 \text{ GeV})$ . The dark photon is introduced by gauging a  $U(1)$  subgroup of the flavor symmetry of this sector so that its mass is generated by the same dynamics as the one forming the dark pion. The model has the following salient features:

- Gauge symmetry of the model does not allow any

mass term for the constituent “dark quarks.” The model, therefore, is fully (i.e. not only technically) natural—the masses of all the new particles arise from the dynamics of new gauge interactions.

- Despite the lack of dark quark masses, all the new particles of the model have nonzero masses. In particular, both the dark pion and dark photon obtain masses of the same order,  $\approx e_D \Lambda / 4\pi$ , where  $e_D$  is the gauge coupling associated with the dark photon.
- The stability of the dark pion is ensured as a result of an accidental symmetry of the model. This accidental symmetry is an extremely good symmetry unless the cutoff scale of the theory is very low.

We find that the model is phenomenologically viable and has interesting implications. In particular,

- There is a significant parameter region in which the dark pion comprises the dark matter of the universe. In this region, the dark pion mass is comparable but smaller than the dark photon mass, which is of order  $10 \text{ MeV} - 1 \text{ GeV}$ . The mixing parameter between the dark and standard model photons is in the range  $\approx 10^{-4.5} - 10^{-2.5}$ .
- In a corner of the allowed parameter region, the discrepancy of the muon  $g - 2$  between the experimental result and standard model prediction [10, 11] is ameliorated due to a loop contribution of the dark photon. Clearly, the model may also ameliorate the muon  $g - 2$  discrepancy even if the dark pion does not comprise all of the dark matter.
- The model predicts a plethora of new resonances around  $10 \text{ MeV} - 10 \text{ GeV}$ , some of which may

	$G_D = SU(N)$	$U(1)_D$	$U(1)_B$	$U(1)_P$
$\Psi_1$	$\square$	1	1	1
$\Psi_2$	$\square$	-1	1	-1
$\bar{\Psi}_1$	$\bar{\square}$	-a	-1	-1
$\bar{\Psi}_2$	$\bar{\square}$	a	-1	1

TABLE I. Charge assignment of the dark quarks under the  $G_D$  and  $U(1)_D$  gauge groups. Here,  $\Psi_{1,2}$  and  $\bar{\Psi}_{1,2}$  are left-handed Weyl spinors. The charges under accidental global symmetries  $U(1)_B$  and  $U(1)_P$  are also shown.

be detectable in future experiments. In particular, one of the lowest-lying spin-one  $C$ - and  $P$ -odd states, the dark rho meson  $\rho_{D_3}$ , mixes with the dark photon and hence couples to the standard model fermions. This provides a monophoton signal, e.g.  $e^+e^- \rightarrow \gamma\rho_{D_3}$ , which can be probed by the Belle II experiment.

The organization of this paper is as follows. In Section II, we present our model and analyze its dynamics. In Section III, we study physics of the dark pion as dark matter. We present a parameter region in which the dark pion is dark matter while avoiding constraints from existing experiments and observations. In Section IV, we discuss the muon  $g-2$ . Finally, in Section V, we discuss the possibility of detecting the dark rho meson.

## II. THE MODEL

The model has a gauge group  $G_D = SU(N)$ , whose dynamical scale (the mass scale of generic low-lying resonances) is  $\Lambda \approx O(10 \text{ MeV} - 1 \text{ GeV})$ , and two flavors of dark quarks transforming under it. In addition, we introduce an Abelian  $U(1)_D$  gauge group under which the dark quarks are charged as in Table I while the standard model particles are singlet. We may take  $0 \leq a \leq 1$  without loss of generality.

We assume  $a \neq 1$ . This makes the theory chiral, i.e. the mass terms of the dark quarks are forbidden by the  $U(1)_D$  gauge symmetry, so that the only free parameters in this sector are the dynamical scale of  $G_D$ ,  $\Lambda$ , and the gauge coupling of  $U(1)_D$ ,  $e_D$ . (There are also  $\theta$  parameters for  $G_D$  and  $U(1)_D$ , but they can be eliminated by phase rotations of dark quarks.) The  $SU(2)_L \times SU(2)_R \times U(1)_B$  flavor symmetry of  $G_D$  is explicitly broken by  $U(1)_D$  gauge interactions. For  $a = 0$  it is broken to  $U(1)_D \times SU(2)_R \times U(1)_B$ , while for  $a \neq 0$  the residual symmetry is  $U(1)_D \times U(1)_B \times U(1)_P$ . (The  $U(1)_B$  symmetry is anomalous with respect to  $U(1)_D$ , but this does not have any consequence for our discussion.) The charges of the dark quarks under  $U(1)_B$  and  $U(1)_P$  are given in Table I.

Let us first discuss the strong dynamics of the dark gauge group  $G_D$ . Below the dynamical scale  $\Lambda$ , the dark

quarks condense,<sup>1</sup>

$$\langle \Psi_1 \bar{\Psi}_1 + \Psi_1^\dagger \bar{\Psi}_1^\dagger \rangle = \langle \Psi_2 \bar{\Psi}_2 + \Psi_2^\dagger \bar{\Psi}_2^\dagger \rangle \neq 0, \quad (1)$$

breaking the axial part of the approximate  $SU(2)_L \times SU(2)_R$  flavor symmetry. The  $U(1)_D$  gauge symmetry is spontaneously broken by this condensation, which can be taken to be real and positive without loss of generality by a phase rotation of dark quark fields. The low energy physics below  $\Lambda$  is thus dictated by three (pseudo and would-be) Nambu-Goldstone bosons  $\pi_i(x)$  ( $i = 1, 2, 3$ ). We define a non-linear sigma model field  $U(x)$  by

$$U(x) = \exp \left[ \frac{i}{f} \sum_{i=1}^3 \pi_i(x) \sigma^i \right]. \quad (2)$$

Here,  $f$  is the decay constant, whose size is given by

$$f \simeq \frac{\sqrt{N}}{4\pi} m_{\rho_D}, \quad (3)$$

where  $m_{\rho_D} \sim \Lambda$  represents the mass of the ‘‘dark rho mesons.’’ The field  $\pi_3$  is the would-be Nambu-Goldstone boson eaten by the  $U(1)_D$  dark photon. Note that  $U(1)_B \times U(1)_P$  remains unbroken by the condensation. The combination  $\phi \equiv (\pi_1 + i\pi_2)/\sqrt{2}$ , which we call the dark pion, comprises a complex scalar field charged under the  $U(1)_P$  symmetry.

The kinetic term and gauge interactions of the dark pion are given by

$$\mathcal{L} = \frac{f^2}{4} \text{tr} [(D_\mu U)(D^\mu U)^\dagger], \quad (4)$$

where

$$D_\mu U = \partial_\mu U - ie_D A_{D\mu} \begin{pmatrix} 1 & \\ & -1 \end{pmatrix} U - ie_D A_{D\mu} U \begin{pmatrix} -a & \\ & a \end{pmatrix}, \quad (5)$$

and  $A_{D\mu}$  is the dark photon field. The mass of  $A_{D\mu}$  is given by

$$m_{A_D} = e_D(1-a)f \simeq \frac{\sqrt{N}}{4\pi} e_D(1-a)m_{\rho_D}, \quad (6)$$

which arises from the dark quark condensation.

For  $a \neq 0$ , the spontaneously broken global symmetry corresponding to  $\phi$  is also explicitly broken by  $U(1)_D$  gauge interactions. The dark pion  $\phi$ , therefore, obtains a mass from quantum corrections due to  $U(1)_D$  gauge interactions in this case. At the lowest order in  $e_D$ , the mass is given by [12]<sup>2</sup>

$$m_\phi^2 \simeq \frac{6a \ln 2}{16\pi^2} e_D^2 m_{\rho_D}^2. \quad (7)$$

<sup>1</sup> The condensation is expected to be in this direction, since  $\Psi_1 \bar{\Psi}_2$  and  $\Psi_2 \bar{\Psi}_1$  have larger  $U(1)_D$  charges than  $\Psi_1 \bar{\Psi}_1$  and  $\Psi_2 \bar{\Psi}_2$ .

<sup>2</sup> In Ref. [12], the electromagnetic current is given by a linear combination of a vector current and the baryon number current. Here we need to include an axial current as well. A possible effect from the nonzero dark photon mass is suppressed by  $(m_{A_D}/m_{\rho_D})^2$ .

From now on, we only consider  $a \neq 0$ .

We next discuss couplings between the dark and standard model sectors. These couplings are induced by a kinetic mixing between the hypercharge,  $U(1)_Y$ , and  $U(1)_D$  gauge bosons, defined by

$$\mathcal{L} = -\frac{1}{4}B_{\mu\nu}B^{\mu\nu} - \frac{1}{4}A_{D\mu\nu}A_D^{\mu\nu} + \frac{1}{2}\frac{\epsilon}{\cos\theta_W}B_{\mu\nu}A_D^{\mu\nu}, \quad (8)$$

where  $B_{\mu\nu}$  and  $A_{D\mu\nu}$  are the  $U(1)_Y$  and  $U(1)_D$  gauge field strengths, and  $\theta_W$  is the Weinberg angle. In the limit  $\epsilon \rightarrow 0$ , the  $Z$  boson and the photon couple to the standard model particles as usual, and the dark photon couples to  $\phi$  through interactions in Eq. (4):

$$\mathcal{L} = (D_\mu\phi)(D^\mu\phi)^\dagger, \quad (9)$$

where

$$D_\mu\phi = \partial_\mu\phi + ie_D(1+a)A_{D\mu}\phi. \quad (10)$$

For  $\epsilon \neq 0$ , after solving the kinetic and mass mixings, we find that the dark photon also couples to standard model particles as [13]

$$\mathcal{L} = -\epsilon e A_{D\mu} J_{\text{em}}^\mu, \quad (11)$$

where  $e$  and  $J_{\text{em}}^\mu$  are the electromagnetic coupling and current, respectively. Here, we have assumed  $m_{A_D} \ll m_Z$  and  $\epsilon \ll 1$ , and neglected interactions suppressed by  $m_{A_D}/m_Z$  or higher powers of  $\epsilon$ . The standard model  $Z$  boson also couples to the  $U(1)_D$  charged particles as

$$\mathcal{L} = \epsilon e_D \tan\theta_W Z_\mu J_D^\mu, \quad (12)$$

where  $J_D^\mu$  is the  $U(1)_D$  current.

Finally, we mention that spontaneous breaking of the  $U(1)_D$  symmetry generates cosmic strings. Observational constraints on them, however, are very weak and do not affect the phenomenology discussed below.

### III. DARK PION AS DARK MATTER

As we have seen, the model has two accidental symmetries  $U(1)_B$  and  $U(1)_P$ . These symmetries guarantee the stability of dark baryons and the dark pion  $\phi$ , respectively. In the early universe, dark baryons effectively annihilate into dark pions, so that their thermal abundance is negligible. We are therefore left with the dark pion as our dark matter candidate.

The  $U(1)_P$  symmetry, in fact, is an extremely good symmetry. The  $G_D$  and  $U(1)_D$  gauge symmetries forbid interactions that explicitly break the  $U(1)_P$  symmetry up to dimension eight. Therefore, unless the scale suppressing higher dimension operators is very low, the dark pion is stable at cosmological timescales.

The phenomenology of the dark particles depends significantly on the ratio of the masses of the dark pion,  $m_\phi$ , and dark photon,  $m_{A_D}$ . Below we discuss three cases  $m_\phi < m_{A_D}/2$ ,  $m_{A_D}/2 < m_\phi < m_{A_D}$ , and  $m_\phi > m_{A_D}$  in turn.

#### 1. $m_\phi < m_{A_D}/2$

The case  $m_\phi < m_{A_D}/2$  occurs if the  $U(1)_D$  charge  $a$  is sufficiently small or if  $N$  is sufficiently large. The thermal abundance of dark pions in this case is determined by the annihilation into standard model particles through  $s$ -channel dark photon exchange. The annihilation cross section into a pair of standard model fermions  $f$  with the electric charge  $q_f$  and mass  $m_f$  is given by

$$\sigma v = \frac{\epsilon^2 q_f^2 (1+a)^2 e^2 e_D^2}{6\pi} \frac{m_\phi^2}{(m_{A_D}^2 - 4m_\phi^2)^2} v^2 \times \left(1 - \frac{m_f^2}{m_\phi^2}\right)^{3/2} \left(1 - \frac{m_f^2}{4m_\phi^2}\right), \quad (13)$$

where  $v$  is the relative velocity between the initial two dark pions. We find that the annihilation cross section is suppressed by the relative velocity. This is because the intermediate dark photon has an odd  $C$  parity and hence the initial state dark pions must be in  $p$ -wave. This implies that the velocity suppression exists regardless of the final state as long as the annihilation is through the  $s$ -channel dark photon exchange.<sup>3</sup>

In Fig. 1, we show the constraints on  $(m_{A_D}, \epsilon)$  for  $m_\phi = 0.4m_{A_D}$  and  $a = 1/2$ . Here, we determine the  $U(1)_D$  gauge coupling,  $e_D$ , so that the thermal relic of dark pions explains the observed dark matter abundance. The blue shaded region in the upper part is excluded by the search for the process  $e^+e^- \rightarrow \gamma + A_D$  at the BaBar experiment [14–16]. The brown shaded region is excluded by the  $K^+ \rightarrow \pi^+\nu\bar{\nu}$  searches at E787 [17] and E949 [18], which constrain the  $K^+ \rightarrow \pi^+A_D$  process [16]. The purple shaded region in the upper-left part is eliminated because of too large contributions to the electron  $g-2$  [19, 20]. The gray shaded region in the left is excluded by the search for the process  $\pi^0 \rightarrow \gamma A_D$  followed by  $A_D \rightarrow \phi\bar{\phi}$  with subsequent scatterings of  $\phi$  in the LSND detector [21, 22]. In the yellow shaded region, dark pions annihilate after neutrinos decouple from the thermal bath in the early universe, so that the neutrino energy density becomes too small [8]. The green shaded region is excluded by the search for the process  $e^-N \rightarrow e^-NA_D$  followed by  $A_D \rightarrow \phi\bar{\phi}$  with subsequent scatterings of  $\phi$  in the E137 detector [23, 24]. Other constraints, such as the one in Ref. [25], do not reduce the allowed parameter space further.

In the region below the gray dashed line, which runs diagonally from the lower left to the upper right, the dark photon coupling is large ( $e_D > 1$  around the dark pion mass scale), so that  $e_D$  hits the Landau pole below typical unification scales of  $10^{14} - 10^{17}$  GeV. If we want

<sup>3</sup> Diagrams with two intermediate dark photons lead to  $s$ -wave annihilation. Such processes are suppressed by  $\epsilon$  and a loop or extra two-body phase space factor, and hence negligible.

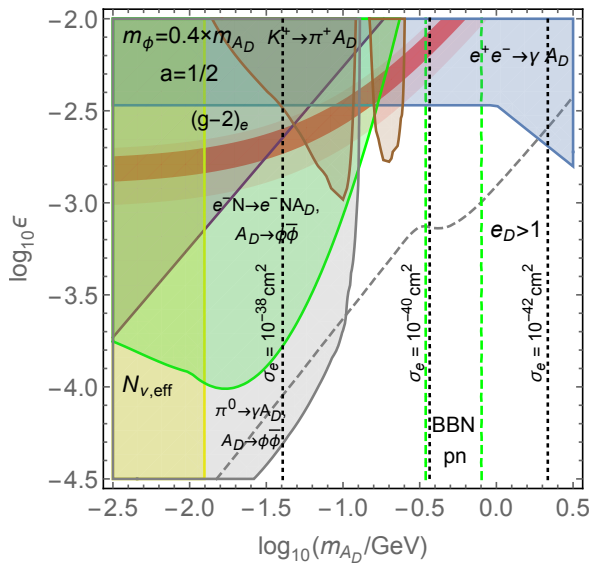


FIG. 1. Constraints on the dark photon mass,  $m_{A_D}$ , and the mixing parameter  $\epsilon$  for  $m_\phi = 0.4m_{A_D}$  and  $a = 1/2$ . The  $U(1)_D$  gauge coupling,  $e_D$ , is determined so that the thermal abundance of dark pions reproduces the observed dark matter abundance. The blue, brown, purple, gray, yellow, and green shaded regions are excluded by the mono-photon search at the BaBar experiment,  $K^+ \rightarrow \pi^+ \nu \bar{\nu}$  searches at E787 and E949, the electron  $g - 2$ , the search for  $\pi^0 \rightarrow \gamma A_D \rightarrow \gamma \phi \bar{\phi}$  with subsequent scatterings of  $\phi$  in the LSND detector, dark pions annihilating after the neutrino decoupling, and the search for  $e^- N \rightarrow e^- N A_D \rightarrow e^- N \phi \bar{\phi}$  with subsequent scatterings of  $\phi$  in the E137 detector, respectively. In the region below the gray dashed line,  $e_D > 1$  around the dark pion mass scale, so that  $e_D$  hits a Landau pole below the unification scale. Between the two vertical green dashed lines, the annihilation of dark pions during the BBN may result in too much  ${}^4\text{He}$ . The calculation of this bound, however, is subject to large theoretical uncertainties; see the text.

to avoid this, we are left with the region centered around  $m_{A_D} \approx O(100 \text{ MeV} - 1 \text{ GeV})$  and  $\epsilon \approx O(10^{-3.5} - 10^{-2.5})$ .

We note that the region between the two vertical green dashed lines may be excluded by the big bang nucleosynthesis (BBN) because annihilations of dark pions into hadrons in the BBN era may lead to proton-nucleon conversion that yields too many  ${}^4\text{He}$  [26, 27]. However, this bound, derived naively by extrapolating the bound in Ref. [27], might be too strong. In Ref. [27], the dark matter mass was taken to be larger than 10 GeV, and the annihilation was assumed to be  $s$ -wave. To convert this to our bound, we first assumed that the upper bound on the dark matter annihilation cross section scales as  $\sigma v \sim m_\phi^{3/2}$  [28]. The factor of  $m_\phi^{3/2}$  comes from the square of the number density of  $\phi$ , and  $m_\phi^{-1/2}$  from the multiplicity of particles produced by the annihilations.<sup>4</sup> We

then adopted the upper bound on the annihilation cross section at the maximum temperature at which the BBN could be affected by the annihilations. This treatment most likely gives a too aggressive bound. For proton-neutron conversion, we assumed the maximum temperature of 1 MeV, where the proton-neutron ratio is fixed in the standard BBN. A precise estimate of the constraint from the BBN requires a dedicated calculation, which is beyond the scope of this paper.

In addition to the bounds discussed above, the annihilation cross section of dark pions is also constrained by the hadro- and photo-dissociation processes during the BBN, effect on fluctuations of the cosmic microwave background, and production of gamma rays in the present universe. Because of the  $p$ -wave suppression of the annihilation, these constraints are weak and do not exclude the parameter region further.

Since the dark pion mass is much smaller than the nucleon mass, it is difficult to directly detect dark pions through collisions with nuclei. However, scattering of dark pions with electrons may be detectable [29]. In Fig. 1, we show the contours of the scattering cross section between the dark pion and the electron, given by

$$\sigma_{\phi e} = \frac{\epsilon^2(1+a)^2 e^2 e_D^2}{2\pi} \frac{m_e^2}{m_{A_D}^4}, \quad (14)$$

in the nonrelativistic and  $m_\phi \gg m_e$  limit. We find that the model gives

$$\sigma_{\phi e} \sim 10^{-42} - 10^{-39} \text{ cm}^2 \text{ for } m_\phi = 0.4m_{A_D}. \quad (15)$$

A projected experiment with semiconductor targets can probe the cross section down to  $\sigma_{\phi e} \sim 10^{-42} \text{ cm}^2$  [29].

## 2. $m_{A_D}/2 < m_\phi < m_{A_D}$

If  $m_{A_D}/2 < m_\phi < m_{A_D}$ , the dark photon does not decay into dark pions. It decays only into standard model fermions. For the annihilation of dark pions, the three-body channel  $\phi\bar{\phi} \rightarrow A_D A_D^* \rightarrow A_D f \bar{f}$  is now open, whose cross section is given by

$$\sigma(\phi\bar{\phi} \rightarrow A_D f \bar{f}) v = \frac{\epsilon^2 q_f^2 (1+a)^4 e^2 e_D^4}{384\pi^3 m_\phi^2} f\left(\frac{m_\phi^2}{m_{A_D}^2}\right). \quad (16)$$

<sup>4</sup> Strictly speaking, the latter scaling is valid only down to  $m_\phi \simeq$

1 GeV, but we also use it below 1 GeV, since the resulting error is expected to be insignificant in the region of interest.

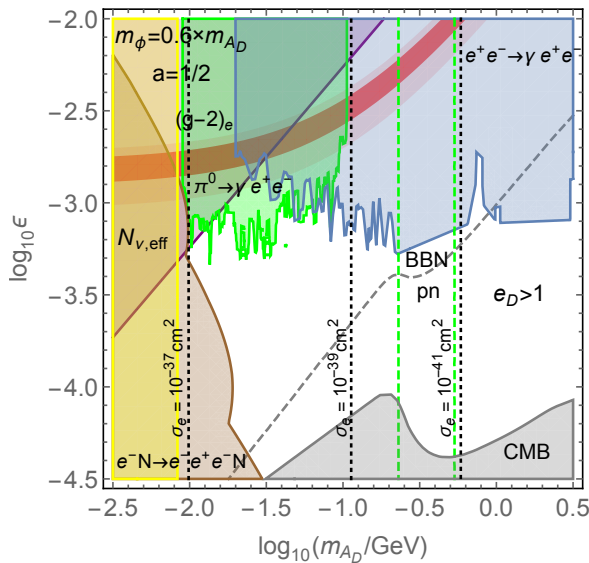


FIG. 2. Constraints on the dark photon mass,  $m_{A_D}$ , and the mixing parameter  $\epsilon$  for  $m_\phi = 0.6m_{A_D}$  and  $a = 1/2$ . The gray shaded region at the bottom is excluded by the constraint from the Planck experiment on the annihilation mode  $\phi\bar{\phi} \rightarrow A_D A_D^* \rightarrow A_D e^+ e^-$ . The blue, green, and brown shaded regions are excluded by the search for the process  $e^+ e^- \rightarrow \gamma A_D \rightarrow \gamma \ell^+ \ell^-$  ( $\ell = e, \mu$ ), the process  $\pi^0 \rightarrow \gamma A_D \rightarrow \gamma e^+ e^-$ , and the process  $e^- N \rightarrow e^- N A_D \rightarrow e^- N e^- e^+$ , respectively. The meanings of the other shaded regions and lines are the same as those in Fig. 1.

Here,

$$\begin{aligned}
 f(x) = & \frac{1}{x(1-2x)^3} \left[ 4(1-4x)(1-2x)(1-3x+4x^2) \right. \\
 & - \sqrt{4x-1}(1-4x)(3-2x) \text{Arctan} \sqrt{4x-1} \\
 & + \frac{1}{\sqrt{1-x}}(3-12x+8x^2)(5-10x+8x^2) \\
 & \times \left( \text{Arctan} \sqrt{\frac{x}{1-x}} + \text{Arctan} \frac{\sqrt{x}-1/2\sqrt{x}}{\sqrt{1-x}} \right) \\
 & \left. + (3-4x)(1-2x)^3 \ln(4x) \right], \quad (17)
 \end{aligned}$$

and we have neglected the mass of the standard model fermion  $f$ . Being the three-body channel, the process is subdominant in determining the thermal abundance of dark pions. It can, however, give dominant effects in later stages of the evolution of the universe, since it is  $s$ -wave. In particular, it is effective around the recombination era and affects the fluctuations of the cosmic microwave background.

Fig. 2 shows the constraints on  $(m_{A_D}, \epsilon)$  for  $m_\phi = 0.6m_{A_D}$  and  $a = 1/2$ . The gray shaded region at the bottom is excluded by the constraint on the annihilation mode  $\phi\bar{\phi} \rightarrow A_D A_D^* \rightarrow A_D e^+ e^-$  from the measurement of the cosmic microwave background by the Planck experiment [7]. The blue, green, and brown shaded regions are excluded by the search for the process  $e^+ e^- \rightarrow \gamma A_D$

followed by  $A_D \rightarrow e^+ e^-, \mu^+ \mu^-$  at the BaBar experiment [30], the search for the process  $\pi^0 \rightarrow \gamma A_D$  followed by  $A_D \rightarrow e^+ e^-$  at the NA48/2 [31], and the search for the process  $e^- N \rightarrow e^- N A_D$  followed by  $A_D \rightarrow e^- e^+$  in beam dump experiments [32], respectively. The meanings of the other shaded regions and lines are the same as those in Fig. 1. This leaves us the region around  $m_{A_D} \approx O(10 \text{ MeV} - 100 \text{ MeV})$  and  $\epsilon \approx O(10^{-4.5} - 10^{-3})$  as the bulk of the viable parameter space. The scattering cross section between the dark pion and the electron in this region is

$$\sigma_{\phi e} \sim 10^{-40} - 10^{-37} \text{ cm}^2 \text{ for } m_\phi = 0.6m_{A_D}. \quad (18)$$

For larger  $m_\phi$ , the three body annihilation mode is more effective because of larger phase space of the final state. As a result, the Planck data becomes more constraining, excluding the model up to larger values of  $\epsilon$ . In particular, for  $m_\phi \gtrsim 0.8m_{A_D}$  no viable parameter region remains.

### 3. $m_\phi > m_{A_D}$

For  $m_\phi > m_{A_D}$ , the thermal abundance of dark pions is determined by the  $s$ -wave annihilation mode of  $\phi\bar{\phi} \rightarrow A_D A_D$ . Since the same annihilation mode is effective in the eras of the BBN and recombination, this mass spectrum is excluded by the constraints from the BBN and the cosmic microwave background.

## IV. MUON $g-2$

The coupling between the muon and the dark photon given by Eq. (11) contributes to the muon  $g-2$  [1, 33]:

$$\Delta a_{\mu, A_D} = \frac{\alpha}{2\pi} \epsilon^2 \int_0^1 dx \frac{2x(1-x)^2 m_\mu^2}{x m_{A_D}^2 + (1-x)^2 m_\mu^2}. \quad (19)$$

In the absence of this contribution, there is a discrepancy of the muon  $g-2$  between the experimental result and standard model prediction,  $a_{\text{exp}} - a_{\text{SM}} = (26.1 \pm 8.0) \times 10^{-10}$  [10, 11]. In Figs. 1 and 2, we depict the region of  $(m_{A_D}, \epsilon)$  in which the experimental and theoretical values become consistent at the  $1\sigma$  ( $2\sigma$ ) level because of this contribution by the red (pink) shaded bands. We find that the regions in which the discrepancy can be ameliorated are excluded by other experiments.

This conclusion, however, does depend on the ratio between the dark pion and dark photon masses. In particular, if  $m_\phi$  is slightly smaller than  $m_{A_D}/2$ , we find a small parameter region in which the muon  $g-2$  discrepancy can be ameliorated. This is because the value of  $e_D$  required to obtain the correct thermal relic abundance becomes smaller for a fixed  $(m_{A_D}, \epsilon)$ , so that the scattering rates of  $\phi$  with the detectors become smaller, weakening constraints. In Fig. 3 we show the same plot as Fig. 1 except that we take  $m_\phi = 0.45m_{A_D}$ , instead of

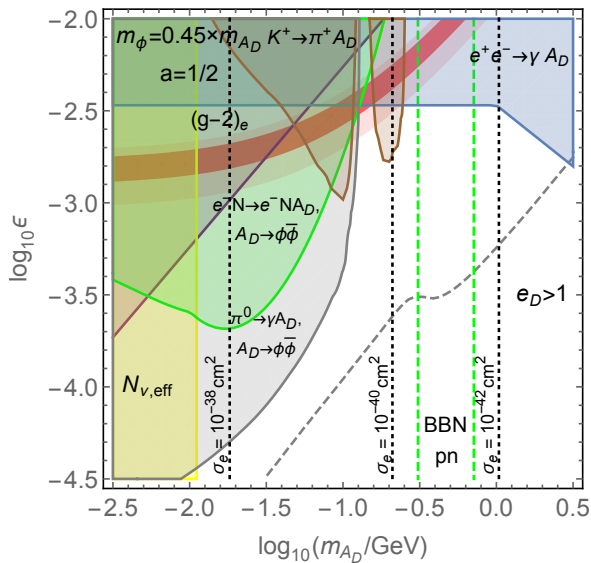


FIG. 3. The same as Fig. 1 except that  $m_{\phi} = 0.45m_{A_D}$ , instead of  $0.4m_{A_D}$ .

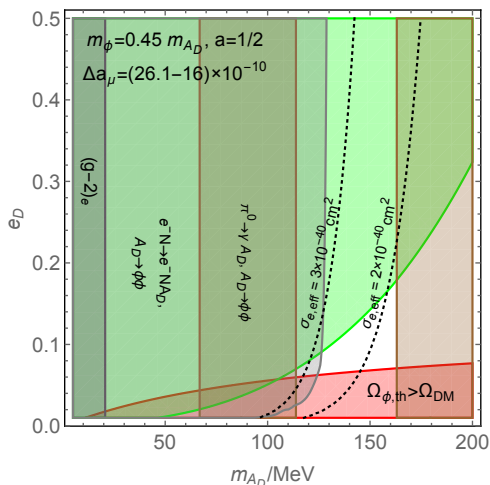


FIG. 4. Constraints on the dark photon mass,  $m_{A_D}$ , and the  $U(1)_D$  gauge coupling,  $e_D$ , for  $m_{\phi} = 0.45m_{A_D}$  and  $a = 1/2$ . The value of the mixing parameter  $\epsilon$  is determined so that  $\Delta a_{\mu, A_D} = (26.1 - 16.0) \times 10^{-10}$ . In the red shaded region, the thermal relic abundance of dark pions exceeds the observed dark matter abundance. The meanings of the other shaded regions are the same as those in Fig. 1. The dotted lines are the contours of the effective scattering cross section between the dark pion and the electron.

$0.4m_{A_D}$ . We see a small region in which the experimental and theoretical values of the muon  $g - 2$  become consistent within  $2\sigma$ . The weakening of the constraints also enlarges the parameter space for dark pion dark matter. In particular, there is now a sliver of the allowed region along the  $e_D \sim 1$  line, which goes down to smaller dark photon masses.

We may consider the model to ameliorate the muon

$g - 2$  discrepancy without requiring that the dark pion comprises all of the dark matter. In Fig. 4, we show the constraints on  $(m_{A_D}, e_D)$  for  $m_{\phi} = 0.45m_{A_D}$  and  $a = 1/2$ , with the value of  $\epsilon$  determined so that the discrepancy of the muon  $g - 2$  between the experimental and standard model values is ameliorated by the dark photon contribution to the  $2\sigma$  level,  $\Delta a_{\mu, A_D} = (26.1 - 16.0) \times 10^{-10}$ . In the red shaded region at the bottom, the thermal relic abundance of dark pions exceeds the observed dark matter abundance. The meanings of the other shaded regions are the same as those in Fig. 1. We find that the discrepancy of the muon  $g - 2$  can be ameliorated in the region around  $m_{A_D} \simeq 150$  MeV, consistently with all the other experiments. In the figure, we also show the contours of the effective scattering cross section between the dark pion and the electron,  $\sigma_{e, \text{eff}} = \sigma_{\phi e} \times (\Omega_{\phi, \text{th}}/\Omega_{\text{DM}})$ .

## V. DARK RHO MESONS

The model predicts a plethora of resonance states composed of the dark quarks and  $G_D$  gauge bosons. The masses of these states depend on parameters of the model but are generally in the range of 10 MeV – 10 GeV. These states may be detectable in various experiments. Here we discuss a possible way to detect the lowest-lying spin-one  $C$ - and  $P$ -odd composite states: the dark rho mesons  $\rho_D$ .

The masses of  $\rho_D$  are expected to be larger than the mass of the dark photon by about an order of magnitude

$$m_{\rho_D} \approx \frac{4\pi}{\sqrt{N}e_D(1-a)} m_{A_D}. \quad (20)$$

One of the dark rho mesons, which we call  $\rho_{D_3}$ , has the same charge as  $\pi_3$  under the vectorial subgroup of  $SU(2)_L \times SU(2)_R$  and mixes with the dark photon. The mixing induces the coupling of  $\rho_{D_3}$  with the standard model fermions

$$\mathcal{L} = \epsilon' \rho_{D_3\mu} J_{\text{em}}^{\mu}, \quad (21)$$

where

$$\epsilon' \approx \frac{\sqrt{N}}{4\pi} e_D \epsilon. \quad (22)$$

This coupling leads to processes such as  $e^+e^- \rightarrow \gamma\rho_{D_3}$ , which yield monophotons. Adopting the analysis for the dark photon in Ref. [16], we find that the Belle II experiment will be sensitive to the dark rho meson with  $\epsilon' \gtrsim 10^{-4}$  for  $1 \text{ GeV} < m_{\rho_{D_3}} < 10 \text{ GeV}$ .<sup>5</sup> Observation of the *two* processes  $e^+e^- \rightarrow \gamma A_D$  and  $\gamma\rho_{D_3}$  in future experiments would provide strong evidence for the model.

<sup>5</sup> In Ref. [16] the width of the dark photon is assumed to be negligible, while our  $\rho_{D_3}$  has a decay width of  $\sim m_{\rho_{D_3}}/N$ . For small  $N$ , this width is not negligible, so that the sensitivity to  $\epsilon'$  would be somewhat weaker. Performing spectroscopy of a dark sector connected with the standard model through  $U(1)$  kinetic mixing has been discussed recently in Ref. [34].

## ACKNOWLEDGMENTS

We thank Hitoshi Murayama for discussion. This work was supported in part by the Director, Office of Sci-

ence, Office of High Energy and Nuclear Physics, of the U.S. Department of Energy under Contract DE-AC02-05CH11231, by the National Science Foundation under grants PHY-1316783 and PHY-1521446, and by MEXT KAKENHI Grant Number 15H05895.

- 
- [1] P. Fayet, Phys. Rev. D **75**, 115017 (2007) [hep-ph/0702176 [hep-ph]].
- [2] M. Pospelov, A. Ritz and M. B. Voloshin, Phys. Lett. B **662**, 53 (2008) [arXiv:0711.4866 [hep-ph]].
- [3] For earlier related work, see M. J. Strassler and K. M. Zurek, Phys. Lett. B **651**, 374 (2007) [hep-ph/0604261].
- [4] D. S. Akerib *et al.* [LUX Collaboration], arXiv:1512.03506 [astro-ph.CO].
- [5] R. Agnese *et al.* [SuperCDMS Collaboration], Phys. Rev. Lett. **116**, 071301 (2016) [arXiv:1509.02448 [astro-ph.CO]].
- [6] C. Boehm, T. A. Enßlin and J. Silk, J. Phys. G **30**, 279 (2004) [astro-ph/0208458]; L. Zhang, X. Chen, Y.-A. Lei and Z.-G. Si, Phys. Rev. D **74**, 103519 (2006) [astro-ph/0603425].
- [7] M. Kawasaki, K. Nakayama and T. Sekiguchi, arXiv:1512.08015 [astro-ph.CO].
- [8] C. Boehm, M. J. Dolan and C. McCabe, JCAP **08**, 041 (2013) [arXiv:1303.6270 [hep-ph]].
- [9] C. Boehm and P. Fayet, Nucl. Phys. B **683**, 219 (2004) [hep-ph/0305261].
- [10] G. W. Bennett *et al.* [Muon g-2 Collaboration], Phys. Rev. D **73**, 072003 (2006) [hep-ex/0602035].
- [11] K. Hagiwara, R. Liao, A. D. Martin, D. Nomura and T. Teubner, J. Phys. G **38**, 085003 (2011) [arXiv:1105.3149 [hep-ph]].
- [12] T. Das, G. S. Guralnik, V. S. Mathur, F. E. Low and J. E. Young, Phys. Rev. Lett. **18**, 759 (1967).
- [13] B. Holdom, Phys. Lett. B **166**, 196 (1986).
- [14] B. Aubert *et al.* [BaBar Collaboration], arXiv:0808.0017 [hep-ex].
- [15] E. Izaguirre, G. Krnjaic, P. Schuster and N. Toro, Phys. Rev. D **88**, 114015 (2013) [arXiv:1307.6554 [hep-ph]].
- [16] R. Essig, J. Mardon, M. Papucci, T. Volansky and Y.-M. Zhong, JHEP **11**, 167 (2013) [arXiv:1309.5084 [hep-ph]].
- [17] S. Adler *et al.* [E787 Collaboration], Phys. Rev. D **70**, 037102 (2004) [hep-ex/0403034].
- [18] A. V. Artamonov *et al.* [E949 Collaboration], Phys. Rev. Lett. **101**, 191802 (2008) [arXiv:0808.2459 [hep-ex]]; Phys. Rev. D **79**, 092004 (2009) [arXiv:0903.0030 [hep-ex]].
- [19] D. Hanneke, S. Fogwell and G. Gabrielse, Phys. Rev. Lett. **100**, 120801 (2008) [arXiv:0801.1134 [physics.atom-ph]]; D. Hanneke, S. F. Hoogerheide and G. Gabrielse, Phys. Rev. A **83**, 052122 (2011) [arXiv:1009.4831 [physics.atom-ph]].
- [20] M. Endo, K. Hamaguchi and G. Mishima, Phys. Rev. D **86**, 095029 (2012) [arXiv:1209.2558 [hep-ph]].
- [21] L. B. Auerbach *et al.* [LSND Collaboration], Phys. Rev. D **63**, 112001 (2001) [hep-ex/0101039].
- [22] B. Batell, M. Pospelov and A. Ritz, Phys. Rev. D **80**, 095024 (2009) [arXiv:0906.5614 [hep-ph]]; P. deNiverville, M. Pospelov and A. Ritz, Phys. Rev. D **84**, 075020 (2011) [arXiv:1107.4580 [hep-ph]].
- [23] J. D. Bjorken *et al.*, Phys. Rev. D **38**, 3375 (1988).
- [24] B. Batell, R. Essig and Z. Surujon, Phys. Rev. Lett. **113**, no. 17, 171802 (2014) [arXiv:1406.2698 [hep-ph]].
- [25] Y. Kahn, G. Krnjaic, J. Thaler and M. Toups, Phys. Rev. D **91**, 055006 (2015) [arXiv:1411.1055 [hep-ph]].
- [26] M. H. Reno and D. Seckel, Phys. Rev. D **37**, 3441 (1988).
- [27] M. Kawasaki, K. Kohri, T. Moroi and Y. Takaesu, Phys. Lett. B **751**, 246 (2015) [arXiv:1509.03665 [hep-ph]].
- [28] B. Henning and H. Murayama, arXiv:1205.6479 [hep-ph].
- [29] R. Essig, J. Mardon and T. Volansky, Phys. Rev. D **85**, 076007 (2012) [arXiv:1108.5383 [hep-ph]].
- [30] J. P. Lees *et al.* [BaBar Collaboration], Phys. Rev. Lett. **113**, 201801 (2014) [arXiv:1406.2980 [hep-ex]].
- [31] J. R. Batley *et al.* [NA48/2 Collaboration], Phys. Lett. B **746**, 178 (2015) [arXiv:1504.00607 [hep-ex]].
- [32] S. Andreas, C. Niebuhr and A. Ringwald, Phys. Rev. D **86**, 095019 (2012) [arXiv:1209.6083 [hep-ph]].
- [33] M. Pospelov, Phys. Rev. D **80**, 095002 (2009) [arXiv:0811.1030 [hep-ph]].
- [34] Y. Hochberg, E. Kuflik and H. Murayama, arXiv:1512.07917 [hep-ph].